

# Enhancement of Wormlike Micellar Structure Induced by *O*-Carboxymethylchitosan with or without Hydrophobic Modifications

Ping Guo and Rong Guo\*

School of Chemistry and Chemical Engineering, Yangzhou University, Yangzhou 225002, People's Republic of China

The enhancement of wormlike micellar structure after the addition of *O*-carboxymethylchitosan (OCMCS) or hydrophobically modified *O*-carboxymethylchitosan (hm-OCMCS) has been studied by rheology and freeze-fracture transmission electron microscopy (FF-TEM). The results show that the viscoelastic properties of the wormlike micelles composed of Tween 80 and Brij 30 increase significantly after the addition of OCMCS. However, as the OCMCS molecules are hydrophobically modified, the viscosity enhancement is reduced and even diminishes with an increase of the length of aliphatic chains. FF-TEM was also used to provide a direct investigation of the microstructure changes of wormlike micelles after the addition of OCMCS and hm-OCMCS. Combined with the rheological behavior of OCMCS and hm-OCMCS, it is speculated that these results originate from a greater degree of intra-aggregation of polymers after hydrophobic modifications, which results in a weaker interaction between polymers and micelles. Additionally, the influence of temperature on the rheological behavior of polymer/wormlike micelle systems also demonstrates the intra-aggregation of polymers is the main impact factor in these systems.

## Introduction

The formation and properties of wormlike micelles have drawn considerable interest in basic research and practical applications.<sup>1–3</sup> In the past two decades, extensive studies have focused on the rheological behavior of wormlike micellar solution containing ionic surfactants and different kinds of binding counterions.<sup>4–7</sup> Recently, the formation of viscoelastic wormlike micellar solutions in nonionic surfactant systems are also receiving much attention.<sup>8,9</sup> Aramaki et al.<sup>10</sup> have investigated the viscoelastic properties of wormlike micelles in Tween 80 aqueous solution with trioxyethylene alkyl ether ( $C_mEO_3$ ,  $m = 12, 14$ , and 16). We also found the formation of wormlike micelles in Tween 80 + Brij 30 ( $C_{12}EO_4$ ) + H<sub>2</sub>O systems.<sup>11</sup>

Wormlike micelles can entangle with each other, forming transient networks and exhibit viscoelastic behavior. However, the structure of these micelles are extremely sensitive to external conditions as shown by the variation of their rheological behavior, because the individual micelles are constantly being destroyed and recreated through Brownian fluctuations. Nowadays, several researchers have already demonstrated that polymers can considerably modify the viscoelasticity of the wormlike micelles.<sup>12,13</sup> Couillet et al.<sup>14</sup> have found the synergistic effects occurring in the viscoelastic behavior of mixtures of 0.4 M KCl aqueous solutions containing erucyl bis-(hydroxyethyl)methylammonium chloride (EHAC) surfactant and hydrophobically modified guar in a concentration domain from (0.01 to 2.5) mass fraction and in a temperature range from (25 to 80) °C. Besides, the addition of some polymers can also decrease the viscosity of wormlike micelles. For example, Suksamranthit et al.<sup>15</sup> have reported that addition of water-soluble polymer polyethylene oxide (PEO) decreases the rheology of HTAC/NaSal solutions. However, most of this research was carried out in ionic surfactant solutions. Only a

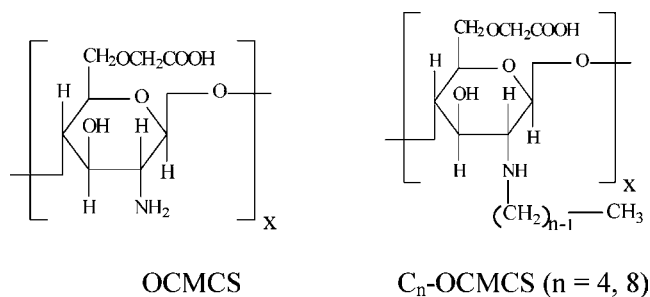
few studies were devoted to polymers interacting with nonionic wormlike micelles, whereas nonionic surfactant systems are receiving much attention these days because growing environmental awareness has stimulated the search for nontoxic and biodegradable surfactants such as polyoxyethylene sorbitan fatty acid esters (Tweens) and sucrose esters. It is believed that knowledge of the structure and dynamics of nonionic wormlike micelles is vital from both environmental and application points-of-view.

*O*-Carboxymethylchitosan (OCMCS) is a derivative of chitosan, and its physicochemical properties are optimized by comparing with chitosan.<sup>16,17</sup> Now, much research has reported that the rheological behavior of hydrophobically modified OCMCS (hm-OCMCS) is different from that of most other polymers, such as hydrophobically modified polyacrylamide or hydroxyethyl cellulose, whose viscosity can be improved by the introduction of hydrophobic groups randomly distributed along the chains.<sup>18–20</sup> For hm-OCMCS, its viscosity decreases with the increasing length of the pendant because the longer hydrophobic pendent promotes the intra-aggregation of the polymer molecules. In recent years, the kind of polymers like hydrophobically modified polyacrylamide has been widely used as thickening agents in wormlike micellar solutions, because the addition of such polymers leads to a stronger synergy in shear flow than that without hydrophobic modification. Here, we want to know if the addition of carboxymethylchitosan and its hydrophobic-modified derivatives, which show different rheological properties, could lead to different results in the mixtures of wormlike micelles and polymers in aqueous solution, and we hope this work could supply some new ideas about how to use polymers to adjust the viscoelastic properties of wormlike micelles.

So, in this paper, we report the influence of OCMCS and hm-OCMCS on the structure of the nonionic wormlike micelles composed of Tween 80 and Brij 30. Actually, the opposite results are obtained in our systems. We find that the addition of OCMCS and hm-OCMCS both increase the viscoelastic

\* Corresponding author. Fax: 86-514-7311374. Tel.: 86-514-7975219. E-mail address: guorong@yzu.edu.cn.

### Scheme 1. Chemical Structures of OCMCS and hm-OCMCS



properties of wormlike micelles at room temperature, but the effect of hm-OCMCS is weaker. This may be attributed to the different intra-aggregate behavior of OCMCS and hm-OCMCS, which results in the variation of interactions between polymer molecules and wormlike micelles.

### Materials and Methods

**Materials.** Polyoxyethylene sorbitan monooleate (Tween 80, 97 %, Sigma) and Brij 30 (> 99 %, Sigma) were all used as received. OCMCS ( $M_w = 2.5 \cdot 10^5$ ; degree of carboxymethyl substitution > 90 %, and degree of deacetylation > 90 %) and chitosan ( $M_w = 2.0 \cdot 10^5$ ; degree of deacetylation > 90 %) of biomedical grade purity were supplied from Qingdao Biochemical Pharmacy Co., China. Water used was deionized and distilled twice.

**Methods. Preparation of Hm-OCMCS.** Hm-OCMCS was synthesized by applying a series of versatile reactions reported previously.<sup>21,22</sup> First, 2.0 g (11.2 mmol) of chitosan (CS) was suspended in 50 mL of methanol, and then 4 g (56 mmol) of butaldehyde or 8 g (56 mmol) of octaldehyde was added in the suspension while stirring at room temperature. After 24 h of reaction, NaBH<sub>4</sub> solution (1.0 g, 26 mmol in 10 mL of water) was slowly added to the reaction mixture. The resulting mixture was stirred at room temperature for another 24 h, and then 2 M HCl was added to it to adjust its pH to 7. After being repeatedly washed with methanol and water, hm-CS was collected by filtration and dried at 50 °C overnight under a reduced pressure. Second, hm-CS was immersed in 50 mL isopropanol containing an appropriate amount of NaOH (about double weight of hm-CS) to swell and alkalize for 24 h. Five grams of monochloroacetic acid was dissolved in 25 mL of isopropanol and then added to above solution for 20 min. After 8 h of reaction, the mixture was filtered to remove the solvent. The filtrate obtained was dissolved in 100 mL of water, and 2 M HCl was added to it to adjust its pH to 7. Then this solution was centrifuged to remove the precipitate, and 400 mL of ethanol was added to precipitate the product. Finally, the product was filtered, rinsed thrice with ethanol, and vacuum-dried at 50 °C. The product structure was confirmed by <sup>1</sup>H NMR and <sup>13</sup>C NMR spectra. The degree of *N*-alkyl and *O*-carboxymethyl substitution were found to be about 60 to 70 and 90 by elemental analysis. The chemical structures of OCMCS and hm-OCMCS are shown in Scheme 1. According to the length of alkyl chain grafted on OCMCS, C<sub>n</sub>-OCMCS was used to express different hm-OCMCS in the following experiments.

**Rheological Measurements.** The rheological measurements were performed in a rheometer Rheostess RS600 (HAAKE RheoStress) at 25 °C using a Couette (cup, DG41, 5.100 mm) for low viscosity solutions and cone-plate geometry (diameter 35 mm and cone angle 1°) for highly viscous gels. Frequency sweeping measurements were performed in the linear viscoelas-

tic regime of the samples, as determined previously by dynamic strain sweeping measurements. The repeatability of this viscometer is better than 99.5 % by performing different sets of measurements of the same substances. The viscosity uncertainty was verified with water at 25 °C, finding that the deviations with the reference data are lower than 1 %. The processes of breaking and reforming of wormlike micelles are determined by the ratio of  $\xi = \tau_{\text{break}}/\tau_{\text{rep}}$ , in which  $\tau_{\text{break}}$  is the average waiting time when the micelle with average length  $L$  is separated into two parts, and  $\tau_{\text{rep}}$  is the time when micelles reform together again. For a quickly separated reaction  $\xi = \tau_{\text{break}}/\tau_{\text{rep}} \ll 1$ , the viscoelastic wormlike micellar solutions behave as a Maxwell fluid described by following equations:<sup>23</sup>

$$G'(\omega) = G_0 \frac{\omega^2 \tau_R^2}{1 + \omega^2 \tau_R^2} \quad (1)$$

$$G''(\omega) = G_0 \frac{\omega \tau_R}{1 + \omega^2 \tau_R^2} \quad (2)$$

where  $G_0$  is the plateau modulus, which is given by  $G'$  at high  $\omega$ ,  $G'$  is the elastic modulus,  $G''$  is the loss modulus, and  $\tau_R$  is relaxation time.

When plotting  $G''$  against  $G'$ , there should be a semicircle called the Cole-Cole plot. It follows that:

$$(G'')^2 + \left(G' - \frac{G_0}{2}\right)^2 = \left(\frac{G_0}{2}\right)^2 \quad (3)$$

Moreover, the zero-shear viscosity ( $\eta_0$ ) is given by the relation:

$$\tau_R = \frac{\eta_0}{G_0} \quad (4)$$

The relaxation time  $\tau_R$  can be estimated at  $(\omega_R)^{-1}$  where  $\omega_R$  is the frequency at which  $G'$  is equal to  $G''$ .

**Fluorescence Experiments.** The steady state emission spectrum of pyrene was performed on a spectrofluorophotometer (RF-5301, Shimadzu Company, Kyoto, Japan) equipped with a thermostat ( $\pm 0.5$  °C). Pyrene was used as the probe to determine if the microenvironmental polarity exists. The respective uncertainties on  $I_1/I_3$  (the intensity ratio of the first peak to the third of the fluorescence spectrum of pyrene) were estimated to be less than 3 %.

**Freeze-Fracture Transmission Electron Microscopy (FF-TEM).** A small amount of sample was placed in a sample cell, and then it was quickly plunged into liquid nitrogen. Then the frozen samples were fractured and replicated in a freeze-fractured apparatus (Balzers BAF 400D). Replicas were examined with a transmission electron microscope (TEM, Tecnai 12 Philip, Holland).

The temperature for this experiment was kept at  $(25 \pm 0.1)$  °C.

### Results and Discussion

**Influence of OCMCS on the Structure of Wormlike Micelles.** In the following experiments,  $w_{\text{Tween80+Brij30}}$  (mass fraction) is fixed at 0.3, and the effects of OCMCS on the structure of wormlike micelles with Tween 80/Brij 30 (mass ratio) = 3.0, 3.5, and 4.0 are discussed respectively.

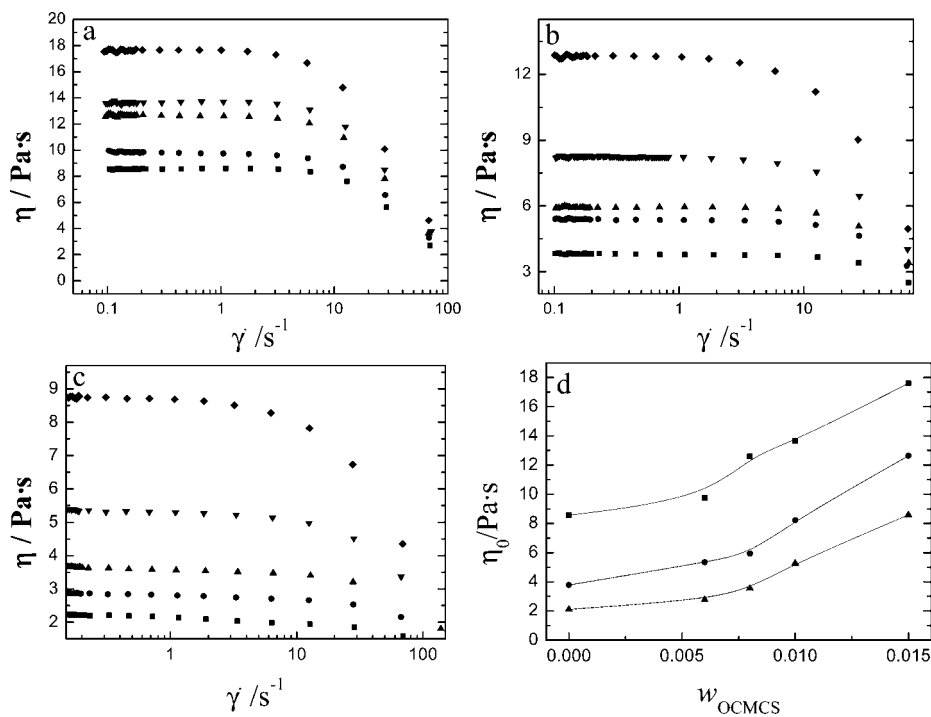


**Figure 1.** Steady shear rate viscosity curves for different  $w_{\text{OCMCS}}$  ( $w_{\text{OCMCS}}$  (mass fraction): ■, 0; ●, 0.006; ▲, 0.008; ▼, 0.01; ◆, 0.014) at Tween 80/Brij 30 (mass ratio) = (a) 3.0, (b) 3.5, (c) 4.0, and  $w_{\text{H}_2\text{O}} = 0.7$  and the corresponding zero-shear viscosity as a function of OCMCS content (d) with Tween 80/Brij 30 (mass ratio) = ■, 3.0; ●, 3.5; ▲, 4.0.

The steady-shear viscosity as a function of shear rate at different mass ratios of Tween 80/Brij 30 in the absence and presence of OCMCS are shown in Figure 1a–c. In the absence of OCMCS, the samples display the typical behavior of wormlike micelles. The viscosity curves are characterized at lower shear rates by a Newtonian plateau, then followed by a shear-thinning region at higher shear rates because the micelles become aligned in the direction of the applied flow.<sup>24–26</sup> The addition of OCMCS has an obvious effect on the viscosity of these samples. As can be seen from Figure 1a–c, the viscosity of wormlike micelles increases sharply with OCMCS content, and the critical shear rate (shear rate at which shear thinning occurs) shifts to lower shear rate region. This indicates that the wormlike micelles become more structured after the addition of OCMCS. The effect of OCMCS on the viscosity of wormlike micelles described in Figure 1a–c is more clearly seen in Figure 1d, where zero shear viscosity,  $\eta_0$ , is plotted as a function of OCMCS content. It can be seen that  $\eta_0$  of the wormlike micelles increases with OCMCS content. When  $w_{\text{OCMCS}}$  (mass fraction) increases to 0.014,  $\eta_0$  is 2 to 3 times of magnitude higher than the pure surfactant solutions. We envisage that the OCMCS chains may wrap around wormlike micelles resulting in the significant viscosity enhancement.

The effect of OCMCS on the viscoelastic properties of the wormlike micelles has been studied by oscillatory shear measurements. Figure 2a–c gives the variation of the elastic modulus ( $G'$ ), and the viscous modulus ( $G''$ ) with oscillation frequency ( $\omega$ ) at different OCMCS contents. All of the samples show a liquid-like behavior ( $G' < G''$ ) at the low frequency region, but both  $G'$  and  $G''$  increase with  $\omega$ , and solid-like behavior ( $G' > G''$ ) is observed at the high frequency region. This is also the typical viscoelastic behavior of wormlike micelles,<sup>27</sup> which is attributed to the entanglement of the wormlike micelles to form a transient network. However, by comparison, the wormlike micelles become more viscous after the addition of OCMCS. As can be seen from Figure 2a–c,  $G'$

and  $G''$  increase with OCMCS content at the low frequency region, and the shear frequencies corresponding to the  $G'$  and  $G''$  crossover,  $\omega_R$ , shift to lower values.  $\omega_R$  is equivalent to the inverse of relaxation time,  $\tau_R$ , which is related to the average length or the network structure of the wormlike micelles.  $\tau_R$  increases with OCMCS content (Figure 2d), indicating the variation of network structure of wormlike micelles after addition of OCMCS. We believe that the long chains of OCMCS may reduce the distance between two separate wormlike micelles by wrapping around the wormlike micelles and result in the formation of more rigid network structures.

To investigate the bridge effect of OCMCS between two micelles clearly, we also studied the influence of OCMCS on the rheology behavior of rod micelles. Steady state shear rate viscosity plots and dynamic rheological measurements for the Tween 80 + Brij 30 systems at various contents of OCMCS are shown in Figure 3, parts a and b, respectively. As can be seen from Figure 3, the viscosity of this sample is much higher than that of a common spherical micellar solution in the absence of OCMCS (Figure 3a), but  $G' - G''$  crossover frequency cannot be measured in dynamic rheological experiments (Figure 3b), implying that there are long rod micelles in this system but the interconnected network is not formed completely. However, after the addition of OCMCS, its viscosity increases greatly (Figure 3a), and when  $w_{\text{OCMCS}}$  (mass fraction) increases to 0.01, a crossover of  $G'$  and  $G''$  ( $\omega_R$ ) is observed at high frequencies (Figure 3b), which shows clearly that OCMCS links the long rod micelles and a complex network is formed.

The interpretation of the complex structures formed was confirmed using FF-TEM. Figure 4a–c shows the FF-TEM images of wormlike micelles at Tween 80/Brij 30 (mass ratio) = 3.0 and  $w_{\text{H}_2\text{O}} = 0.7$  (mass fraction) in the absence and presence of OCMCS. From these figures, we can see that the addition of OCMCS promotes the network structure of wormlike micelles, suggesting the polymer chains may wrap around the wormlike micelles to form complex network structures. This is

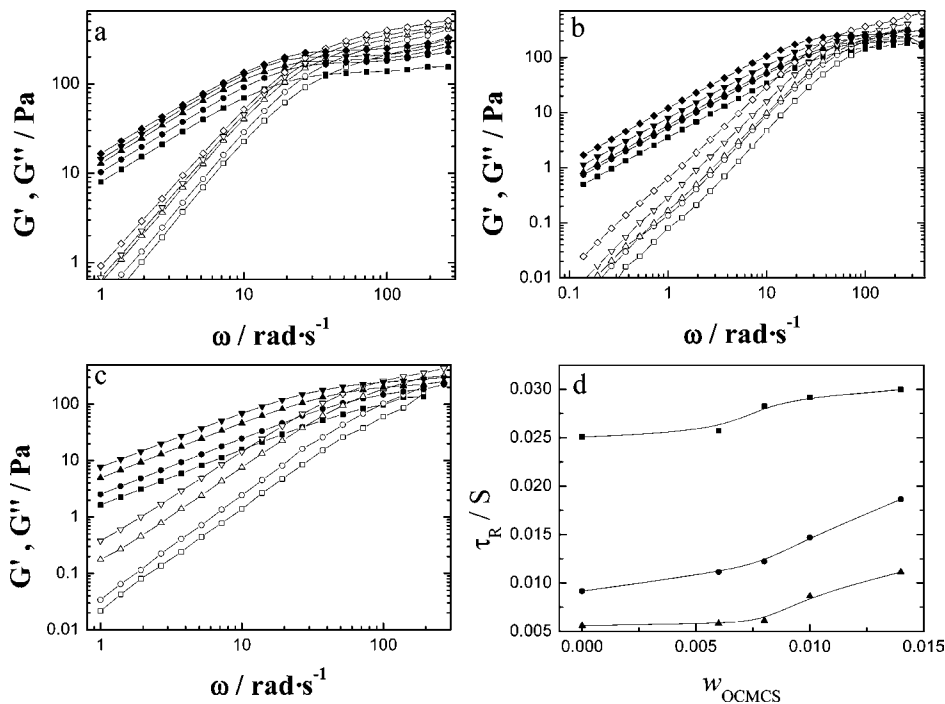


**Figure 2.** Variation of elastic modulus,  $G'$  (open symbols), and viscous modulus,  $G''$  (filled symbols), as a function of oscillatory-shear frequency ( $\omega$ ) at Tween 80/Brij 30 (mass ratio) = (a) 3.0, (b) 3.5, (c) 4.0, and  $w_{\text{H}_2\text{O}} = 0.7$  ( $w_{\text{OCMCS}}$  (mass fraction): (a, b)  $\blacksquare, \square, 0$ ;  $\bullet, \circ, 0.006$ ;  $\blacktriangle, \triangle, 0.008$ ;  $\blacktriangledown, \triangledown, 0.01$ ;  $\blacklozenge, \lozenge, 0.014$ ); (c)  $\blacksquare, \square, 0$ ;  $\bullet, \circ, 0.008$ ;  $\blacktriangle, \triangle, 0.01$ ;  $\blacktriangledown, \triangledown, 0.014$ ) and the corresponding  $\tau_R$  as a function of  $w_{\text{OCMCS}}$  (d) with Tween 80/Brij 30 (mass ratio) =  $\blacksquare, 3.0$ ;  $\bullet, 3.5$ ;  $\blacktriangle, 4.0$ .

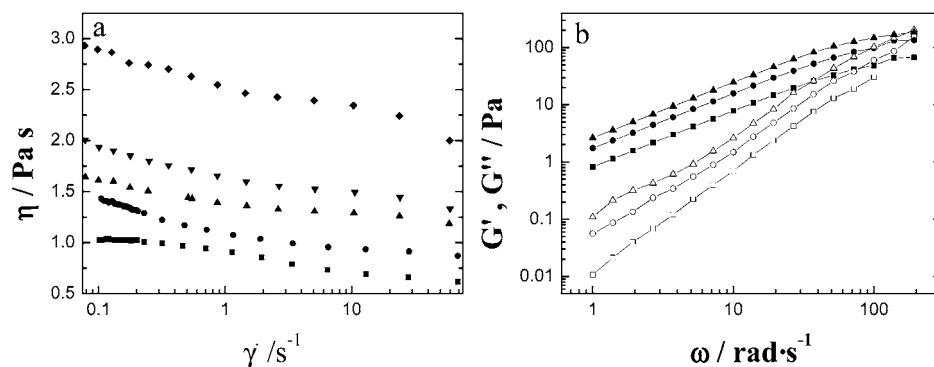


**Figure 3.** (a) Steady shear rate viscosity curves for different  $w_{\text{OCMCS}}$  ( $w_{\text{OCMCS}}$  (mass fraction):  $\blacksquare, 0$ ;  $\bullet, 0.006$ ;  $\blacktriangle, 0.008$ ;  $\blacktriangledown, 0.01$ ;  $\blacklozenge, 0.014$ ). (b) Variation of elastic modulus,  $G'$  (open symbols), and viscous modulus,  $G''$  (filled symbols), as a function of oscillatory-shear frequency ( $\omega$ ) ( $w_{\text{OCMCS}}$  (mass fraction):  $\blacksquare, 0$ ;  $\bullet, 0.01$ ;  $\blacktriangle, 0.014$ ) at Tween 80/Brij 30 (mass ratio) = 5.0 and  $w_{\text{H}_2\text{O}} = 0.7$  (mass fraction).

consistent with the analysis of rheology data. Moreover, the polymer chains act as physical cross-links can be seen more clearly from Figure 4d–f. Figure 4d shows the FF-TEM image of long rod micelles, and the network structure is not formed. But, after the addition of OCMCS, the complex network structure is observed (Figure 4e,f).

**Influence of hm-OCMCS on the Structure of Wormlike Micelles.** Philippova et al.<sup>12</sup> have concluded that hydrophilic polymers that contain some hydrophobic segments always have an obvious effect on surfactant aggregates, because such polymers prefer to reside in water and contact with micelles only by hydrophobic units. Addition of such polymers to micelles always increases its viscosity greatly. Here, the linear aliphatic chains were grafted on the OCMCS backbone, but the physical linking effect of alkyl chains is not observed.

We find that the addition of hm-OCMCS has little discernible influence on the viscosity of wormlike micelles (Figure S1 in the Supporting Information). At lower content of hm-OCMCS, the viscosity shows no systematic variation. When  $w_{\text{hm-OCMCS}}$  (mass fraction) increases to 0.005 or above, a small increase in

viscosity is observed, and ultimately a phase separation occurred (Figure 5a). Compared with the results obtained in OCMCS/wormlike micelles mixtures under the comparable conditions, which is also shown in Figure 5a, we find that as the OCMCS molecules are hydrophobically modified, the viscosity enhancement is reduced, and the enhancement diminishes with an increase of the length of aliphatic chain. The same results are attained at Tween 80/Brij 30 (mass ratio) = 3.5 and 4.0. So, we suspect that there are no efficient hydrophobic interactions between micelles and alkyl chains on hm-OCMCS, which may be attributed to the greater degree of intra-aggregation of polymers after hydrophobic modifications. In general, polymers after hydrophobically modified (hm-polymers) have the capability of forming interacting networks in solution through associations between the hydrophobic side chains from different polymer molecules (i.e., hydrophobic associations), thereby inducing viscosity increase. But, chitosan or its derivatives are special. Ortona et al.<sup>28</sup> have studied the aggregation behavior of hydrophobically modified chitosan in aqueous solution. In that paper, linear aliphatic chains of length variable from 5 to

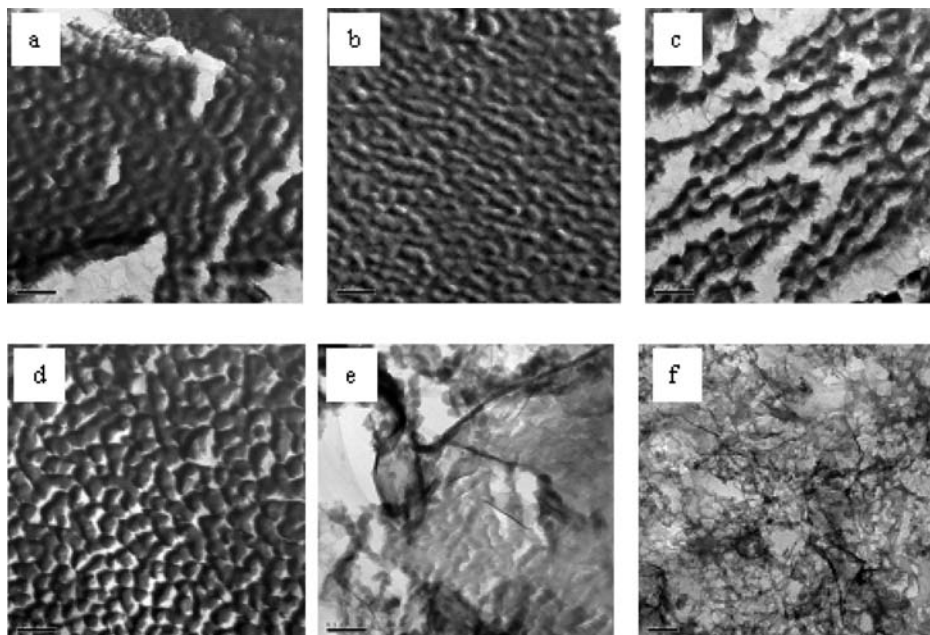


**Figure 4.** Freeze-fractured images of micelles at Tween 80/Brij 30 (mass ratio) = (a–c) 3.0; (d–f) 5.0; and  $w_{\text{H}_2\text{O}} = 0.7$  (mass fraction) in the absence (sample a and d) and presence of OCMCS ( $w_{\text{OCMCS}}$  (mass fraction): 0.006 in sample b and e, 0.01 in sample c and f).

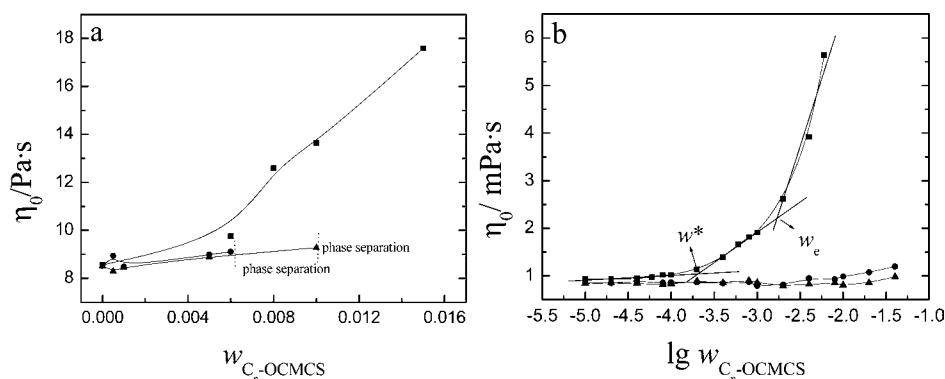


**Figure 5.** Zero-shear viscosity of polymer/wormlike micelle systems (a) and polymer solutions (b). (a, b) ■, OCMCS; ●,  $C_4$ -OCMCS; ▲,  $C_8$ -OCMCS.

12 carbon atoms have been grafted on the chitosan backbone by amination reaction. They find that for  $C_6$ ,  $C_8$ , and  $C_{10}$  chitosan, the increasing length of the pendant promotes intra-aggregation of the polymer molecules and the aggregation becomes compact as shown by the reduction of its hydrodynamic radius. A similar result has been found here. As can be seen from Figure 5b, the viscosity of OCMCS solution shows three different scaling regions. The compositions corresponding to the two breaks in the viscosity curve are overlap composition ( $w^* = 0.0002$ ), which is the polymer composition at which chains start overlapping, and entanglement composition ( $w_c = 0.002$ ), above which the chain dimensions form entanglements. So, above entanglement composition, the viscosity of OCMCS solution increases sharply. However, the solution viscosity of hm-OCMCS increases slowly in the studied content region, and the viscosity value is not only much lower than that of OCMCS but also shows a descending trend with increasing the length of the aliphatic chains, suggesting a shrinking effect of the polymer chains driven by the hydrophobic interaction of alkyl chains. From a general viewpoint, if the intramolecular hydrophobic interactions of polymer chains were strengthened, the intermolecular interactions of polymers and other molecules would be weakened. So, the magnitude of viscosity follows the order:  $\eta_{\text{OCMCS/wormlikemicelles}} > \eta_{C_4\text{-OCMCS/wormlikemicelles}} > \eta_{C_8\text{-OCMCS/wormlikemicelles}} > \eta_{\text{wormlikemicelles}}$  (the schematic representa-

tion of the interactions between OCMCS/hm-OCMCS and wormlike micelles is shown in Figure 6).

FF-TEM was also used to investigate the microstructure changes of mixed micelles after the addition of hm-OCMCS (Figure 7). Compared with Figure 7a–c, we find that complex networks are also formed in hm-OCMCS/wormlike micelle systems. But, compared with OCMCS/wormlike micelle systems, it seems the network structure of hm-OCMCS/wormlike micelles is less compact, which is consistent with above rheological data.

**Effect of Temperature on the Structure of Polymer/Wormlike Micelles Systems.** From above experiments, we conclude that the different intra-aggregation behaviors of OCMCS and hm-OCMCS are the main reason inducing the different rheological behavior of polymer/wormlike micelles systems. A study of the effect of temperature on the rheological behavior of polymer/wormlike micelle systems also demonstrates our explanation, because temperature is still an important parameter that affects the aggregation of polymers.

Figure 8 allows us to compare the dependencies of the viscosity of wormlike micelles on temperature in the absence and presence of polymers. It can be seen that the trend of the  $\eta_0-t$  curve remains the same after the addition of polymers. When the temperature is increased,  $\eta_0$  first increases to a maximum, then followed by a sharp decrease. It is speculated

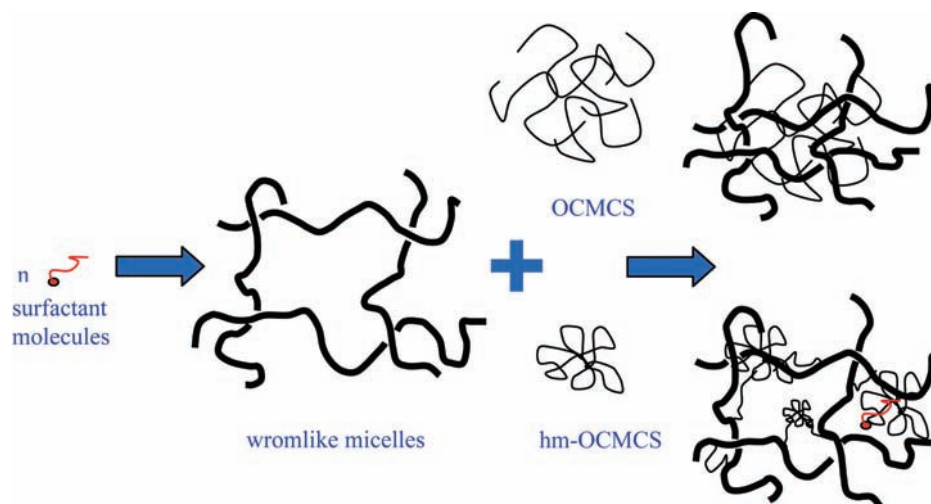


Figure 6. Schematic representation of the interactions between OCMCS/hm-OCMCS and wormlike micelles.

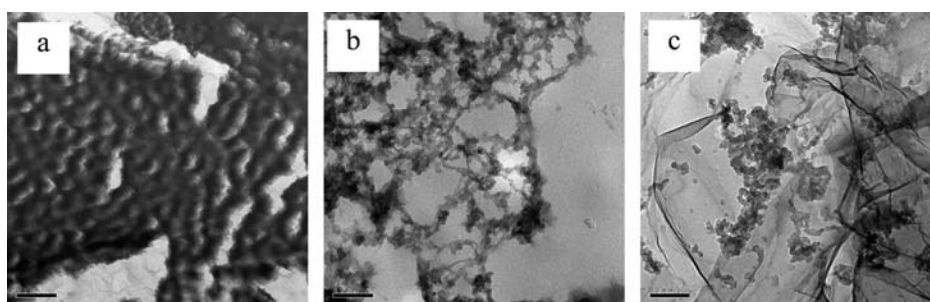


Figure 7. Freeze-fractured images of micelles at Tween 80/Brij 30 (mass ratio) = 3.0 and  $w_{\text{H}_2\text{O}} = 0.7$  (mass fraction) in the absence (sample a) and presence of  $\text{C}_4$ -OCMCS ( $w_{\text{C}_4\text{-OCMCS}}$  (mass fraction): 0.006 in sample b) and  $\text{C}_8$ -OCMCS ( $w_{\text{C}_8\text{-OCMCS}}$  (mass fraction): 0.01 in sample c).

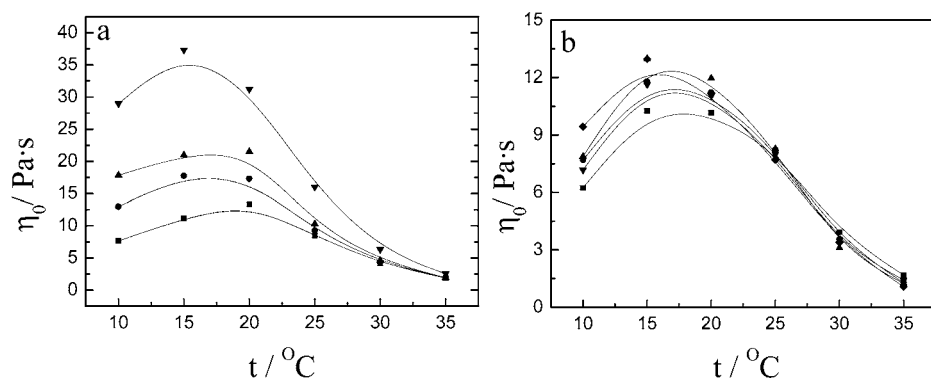
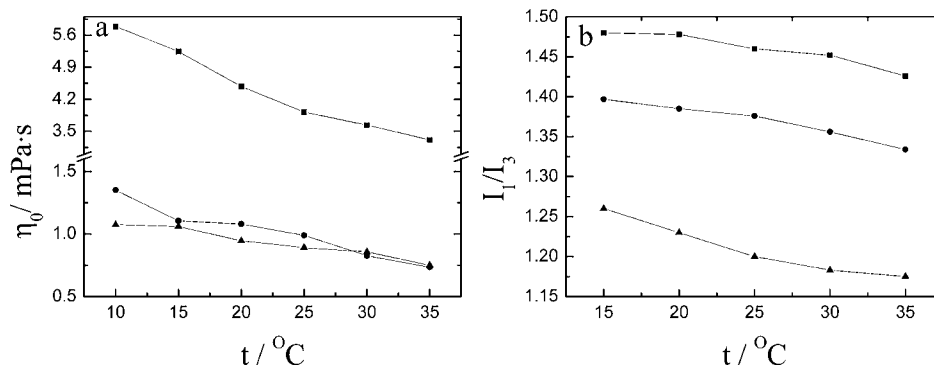


Figure 8. Variation of zero-shear viscosity with temperature at Tween 80/Brij 30 (mass ratio) = 3.0 and  $w_{\text{H}_2\text{O}} = 0.7$  (mass fraction). (a)  $w_{\text{OCMCS}}$  (mass fraction): ■, 0; ●, 0.002; ▲, 0.006; ▼, 0.01. (b)  $w_{\text{C}_4\text{-OCMCS}}$  (mass fraction): ■, 0; ●, 0.002; ▲, 0.006;  $w_{\text{C}_8\text{-OCMCS}}$  (mass fraction): ▼, 0.002; ◆, 0.006.

that there are two factors that should be considered in this process.<sup>29</sup> First, as the temperature increases, the extent of hydration of the EO groups of surfactant molecules decreases, which reduces the average area of amphiphile molecules on the micellar surface, and then decreases the spontaneous curvature of micelles. Hence, the extent of micellar growth increases, resulting in the increase of  $\eta_0$ . Second, the scission of the wormlike micelles also becomes favored with increasing temperature, thus decreasing the viscosity of the system. For a nonionic surfactant, such as Tween 80 and Brij 30, the hydration of the oxyethylene unit is sensitive to the temperature, and this effect on the micellar growth opposes that of micellar scission. Consequently, the decreased interfacial curvature is the main factor at lower temperature, and  $\eta_0$  increases. The contribution of micellar scission becomes significant at higher temperatures. So, the viscosity of the solution decreases, and eventually the wormlike micellar behavior is lost.

Besides, compared with Figure 8 parts a and b, we find another similar phenomenon. Although the influence of hm-OCMCS is weaker than that of OCMCS, the additions of OCMCS and hm-OCMCS both lead to a larger increase in viscosity at lower temperature, and with increasing the temperature, the enhancement of the viscosity becomes smaller. We suspect that the disruption of H-bonding interaction of polymer and surfactant molecules at higher temperature is one of the reasons in this process. The variation of aggregation behavior of polymers at different temperatures is another important factor. As can be seen from Figure 9a,  $\eta_0$  of both OCMCS and hm-OCMCS solution decreases by increasing temperature, implying that the OCMCS/hm-OCMCS aggregates become more compact. This is further confirmed by pyrene  $I_1/I_3$  against temperature in polymer solutions (Figure 9b). It is well-known that the intensity ratio of the first peak to the third ( $I_1/I_3$ ) of the fluorescence spectrum of pyrene shows the microenvironmental



**Figure 9.** Variation of zero-shear viscosity (a) and  $I_1/I_3$  of pyrene (b) with temperature in OCMCS ( $w_{\text{OCMCS}} = 0.005$ ) (■) and  $C_n$ -OCMCS ( $w_{C_n\text{-OCMCS}} = 0.005$ ) (●,  $C_4$ -OCMCS; ▲,  $C_8$ -OCMCS) solutions.

**Table 1.** Value of Flow Activation Energy of Wormlike Micelles with Different  $w_{\text{OCMCS}}$  or  $w_{C_n\text{-OCMCS}}$

| $w$ (OCMCS or $C_n$ -OCMCS) | $E_\eta$<br>kJ·mol <sup>-1</sup> |
|-----------------------------|----------------------------------|
| 0                           | 95.838                           |
| 0.002 (OCMCS)               | 110.494                          |
| 0.005 (OCMCS)               | 120.555                          |
| 0.01 (OCMCS)                | 126.632                          |
| 0.002 ( $C_4$ -OCMCS)       | 109.674                          |
| 0.005 ( $C_4$ -OCMCS)       | 116.301                          |
| 0.002 ( $C_8$ -OCMCS)       | 104.917                          |
| 0.005 ( $C_8$ -OCMCS)       | 117.321                          |

polarity where the probe exists. It appears that  $I_1/I_3$  decreases sharply with increasing temperature, suggesting that a more hydrophobic region is formed because of the shrinkage of polymer chains. So we speculate that a greater degree of intra-aggregation of polymer chains leads to a weaker interaction between polymer chains and wormlike micelles at higher temperature and then results in  $\eta_0$  scarcely increasing with OCMCS/hm-OCMCS content.

In above systems, we also find that, at higher temperatures,  $\eta_0$  decreases exponentially with temperature (Figure S2 in the Supporting Information), which is in accordance with the Arrhenius equation,<sup>30</sup>

$$\log \eta_0(T) = \log K + \frac{E_\eta}{2.303RT} \quad (5)$$

where  $E_\eta$  is the flow activation energy,  $R$  is the universal gas constant, and  $K$  is a constant. The value of flow activation energy can be calculated from the slope of the straight line, and the results are shown in Table 1. As can be seen from Table 1, after the addition of OCMCS or hm-OCMCS, the value of flow activation energy becomes larger, which indicates that polymer chains can link the wormlike micelles, resulting in a higher resistance to flow and consequently a higher activation energy for flow. But, compared with OCMCS/wormlike micelle mixtures,  $E_\eta$  is smaller in hm-OCMCS/wormlike micelle mixtures, which suggests that the interaction between OCMCS and wormlike micelles is stronger and the complex network is more rigid. This is consistent with the results obtained in above rheology experiments.

## Conclusions

In a word, intra-aggregation behavior of OCMCS and hm-OCMCS is the main impact factor in our experiments. Because the grafted alkyl chains promote the intra-aggregation of hm-OCMCS, the aggregation of hm-OCMCS becomes more

compact than that of OCMCS, which results in the weaker interactions between hm-OCMCS chains and surfactant molecules. So, although the additions of OCMCS and hm-OCMCS to wormlike micelles both lead to the formation of more rigid complex network structures at room temperature, the effect of hm-OCMCS is weaker. FF-TEM images show the complex network structures clearly.

Temperature is also an important factor that can influence the aggregation behavior of polymer molecules. At lower temperature, the OCMCS and hm-OCMCS chains are looser, which favors the intermolecular interactions between polymer chains and micelles. Hence, a larger increase in viscosity can be observed at lower temperature.

## Supporting Information Available:

Steady shear rate viscosity curves and zero shear viscosity versus  $1/T$  in Figures S1 and S2, respectively. This material is available free of charge via the Internet at <http://pubs.acs.org>.

## Literature Cited

- Walker, L. M. Rheology and structure of worm-like micelles. *Curr. Opin. Colloid Interface Sci.* **2001**, *6*, 451–456.
- Sharma, S. C.; Acharya, D. P.; Aramaki, K. Viscoelastic Micellar Solutions in a Mixed Nonionic Fluorinated Surfactants System and the Effect of Oils. *Langmuir* **2007**, *23*, 5324–5330.
- Raghavan, S. R.; Kaler, E. W. Highly Viscoelastic Wormlike Micellar Solutions Formed by Cationic Surfactants with Long Unsaturated Tails. *Langmuir* **2001**, *17*, 300–306.
- Kumar, S.; Bansal, D.; Kabir-ud-Din. Micellar Growth in the Presence of Salts and Aromatic Hydrocarbons: Influence of the Nature of the Salt. *Langmuir* **1999**, *15*, 4960–4965.
- Zheng, Y.; Lin, Z.; Zakin, J. L.; Talmon, Y.; Davis, H. T.; Scriven, L. E. Cryo-TEM Imaging the Flow-Induced Transition from Vesicles to Threadlike Micelles. *J. Phys. Chem. B* **2000**, *104*, 5263–5271.
- Cao, Q.; Yu, L.; Zheng, L. Q.; Li, G. Z.; Ding, Y. H.; Xiao, J. H. Rheological properties of wormlike micelles in sodium oleate solution induced by sodium ion. *Colloids Surf., A* **2008**, *312*, 32–38.
- Torres, M. F.; González, J. M.; Rojas, M. R.; Müller, A. J.; Sáez, A. E.; Löf, D.; Schillén, K. Effect of ionic strength on the rheological behavior of aqueous cetyltrimethylammonium *p*-toluene sulfonate solutions. *J. Colloid Interface Sci.* **2007**, *307*, 221–228.
- Acharya, D. P.; Kunieda, H. Formation of Viscoelastic Wormlike Micellar Solutions in Mixed Nonionic Surfactant Systems. *J. Phys. Chem. B* **2003**, *107*, 10168–10175.
- Koehler, R. D.; Raghavan, S. R.; Kaler, E. W. Microstructure and Dynamics of Wormlike Micellar Solutions Formed by Mixing Cationic and Anionic Surfactants. *J. Phys. Chem. B* **2000**, *104*, 11035–11044.
- Varade, D.; Ushiyama, K.; Shrestha, L. K.; Aramaki, K. Wormlike micelles in Tween-80/ $C_m$ EO<sub>3</sub> mixed nonionic surfactant systems in aqueous media. *J. Colloid Interface Sci.* **2007**, *312*, 489–497.
- Yue, H.; Guo, P.; Guo, R. Wormlike Micelles in Tween 80/Brij 30 Mixed Nonionic Surfactant Systems in Aqueous Media (unpublished).
- Shashkina, J. A.; Philippova, O. E.; Zoroslov, Y. D.; Khokhlov, A. R.; Pryakhina, T. A.; Blagodatskikh, I. V. Rheology of Viscoelastic Solutions of Cationic Surfactant. Effect of Added Associating Polymer. *Langmuir* **2005**, *21*, 1524–1530.

- (13) Ramos, L.; Ligoure, C. Structure of a New Type of Transient Network: Entangled Wormlike Micelles Bridged by Telechelic Polymers. *Macromolecules* **2007**, *40*, 1248–1251.
- (14) Couillet, I.; Hughes, T.; Maitland, G. Synergistic Effects in Aqueous Solutions of Mixed Wormlike Micelles and Hydrophobically Modified Polymers. *Macromolecules* **2005**, *38*, 5271–5282.
- (15) Suksamranchit, S.; Sirivat, A.; Jamieson, A. M. Influence of polyethylene oxide on the rheological properties of semidilute, wormlike micellar solutions of hexadecyltrimethylammonium chloride and sodium salicylate. *J. Colloid Interface Sci.* **2006**, *304*, 497–504.
- (16) Zhu, A. P.; Fang, N. Adhesion dynamics, morphology, and organization of 3T3 fibroblast on chitosan and its derivative: the effect of O-carboxymethylation. *Biomacromolecules* **2005**, *6*, 2607–2614.
- (17) Cai, K.; Yao, K.; Li, Z.; Yang, Z.; Li, X. Rat osteoblast functions on the *o*-carboxymethyl chitosan-modified poly(D,L-lactic acid) surface. *J. Biomater. Sci. Polym. Educ.* **2001**, *12*, 1303–1315.
- (18) Ng, W. K.; Tam, K. C.; Jenkins, R. D. Rheological properties of methacrylic acid/ethyl acrylate copolymer: Comparison between unmodified and hydrophobically modified systems. *Polymer* **2001**, *42*, 249–259.
- (19) Xue, W.; Hamley, I. W.; Castelletto, V.; Olmsted, P. D. Synthesis and characterization of hydrophobically modified polyacrylamides and some observations on rheological properties. *Eur. Polym. J.* **2004**, *40*, 47–56.
- (20) Rojas, M. R.; Müller, A. J.; Sáez, A. E. Synergistic effects in flows of mixtures of wormlike micelles and hydroxyethyl celluloses with or without hydrophobic modifications. *J. Colloid Interface Sci.* **2008**, *322*, 65–72.
- (21) Zhang, C.; Ding, Y.; Ping, Q. N.; Yu, L. L. Novel Chitosan-Derived Nanomaterials and Their Micelle-Forming Properties. *J. Agric. Food Chem.* **2006**, *54*, 8409–8416.
- (22) Zhu, A. P.; Chan-Park, M. B.; Dai, S.; Li, L. The aggregation behavior of O-carboxymethylchitosan in dilute aqueous solution. *Colloids Surf., B* **2005**, *43*, 143–149.
- (23) Kunieda, H.; Kabir, H.; Aramaki, K.; Shigeta, K. Phase behavior of mixed polyoxyethylene-type nonionic surfactants in water. *J. Mol. Liq.* **2001**, *90*, 157–166.
- (24) Acharya, D. P.; Hattori, K.; Sakai, T.; Kunieda, H. Phase and rheological behavior of salt-free alkyltrimethylammonium bromide/alkanoyl-N-methylethanolamide/water systems. *Langmuir* **2003**, *19*, 9173–9178.
- (25) Flood, C.; Dreiss, C. A.; Croce, V.; Cosgrove, T. Wormlike Micelles Mediated by Polyelectrolyte. *Langmuir* **2005**, *21*, 7646–7652.
- (26) Croce, V.; Cosgrove, T.; Dreiss, C. A.; King, S.; Maitland, G.; Hughes, T. Giant micellar worms under shear: a rheological study using SANS. *Langmuir* **2005**, *21*, 6762–6768.
- (27) Nettesheim, F.; Liberatore, M. W.; Hodgdon, T. K.; Wagner, N. J.; Kaler, E. W.; Vethamuthu, M. Influence of Nanoparticle Addition on the Properties of Wormlike Micellar Solutions. *Langmuir* **2008**, *24*, 7718–7726.
- (28) Ortona, O.; Errico, G. D.; Mangiapia, G.; Ciccarelli, D. The aggregative behavior of hydrophobically modified chitosans with high substitution degree in aqueous solution. *Carbohydr. Polym.* **2008**, *74*, 16–21.
- (29) Acharya, D. P.; Varade, D.; Aramaki, K. Effect of temperature on the rheology of wormlike micelles in a mixed surfactant system. *J. Colloid Interface Sci.* **2007**, *315*, 330–336.
- (30) Shrestha, R. G.; Shrestha, L. K.; Aramaki, K. Wormlike micelles in mixed amino acid-based anionic/nonionic surfactant systems. *J. Colloid Interface Sci.* **2008**, *322*, 596–604.

Received for review June 1, 2010. Accepted August 9, 2010. This research work was supported by the National Nature Science Foundation of China (Nos. 20633010 and 20773106).

JE100611Z